Journal of Alloys and Compounds 507 (2010) 225–229

Contents lists available at ScienceDirect

Journal of Alloys and Compounds

journal homepage: www.elsevier.com/locate/jallcom

Synthesis of electrospun ZnO/CuO nanocomposite fibers and their dielectric and non-linear optic studies

G. Nixon Samuel Vijayakumar[a,b], S. Devashankar[b], M. Rathnakumari[b], P. Sureshkumar[c,*]

[a] Department of Physics, R.M.K. Engineering College, R.S.M. Nagar, Kavaraipettai 601206, India
[b] Materials Research Centre, Department of Physics, Velammal Engineering College, Chennai 600066, TN, India
[c] Department of Physics, Saveetha School of Engineering, Saveetha University, Thandalam, Chennai 602105, India

ARTICLE INFO

Article history:
Received 19 April 2010
Received in revised form 20 July 2010
Accepted 22 July 2010
Available online 4 August 2010

Keywords:
Composite material
Sol–gel process
Non-linear optics
Scanning electron microscopy

ABSTRACT

The blend of sol–gel processing and electrospinning technique, yields composite nanofibers of poly(vinyl alcohol) (PVA)/zinc acetate/copper acetate. Calcining these fibers resulted in nanocomposite fibers of ZnO/CuO with diameters of 50–100 nm which was revealed by the scanning electron microscope images. Energy dispersive X-ray analysis (EDX) confirmed the presence of the ZnO/CuO composite. The synthesized materials have been also characterized by Fourier transform infrared spectroscopy (FTIR), ultraviolet–visible–near-infrared spectroscopy (UV–vis–NIR) and powder X-ray diffraction (XRD). From the UV spectra, the band gap of the nanocomposite was calculated to be 3.1 eV. Dielectric properties of these samples at different temperatures were studied with respect to frequency. The second harmonic generation efficiency of the material was found to be 11.1 times that of potassium dihydrogen orthophosphate (KDP).

1. Introduction

In recent years, nanomaterials research has gained greater momentum due to their possession of enthralling magnetic, thermo electric, optic, catalytic and mechanical properties [1–5]. Numerous methods have been recommended for the synthesis of such materials including mechanical alloying, sol–gel process, chemical vapor deposition (CVD), microwave synthesis, metal-organic CVD technique (MOCVD), co-precipitation method and facile route synthesis approach [4–10]. One dimensional nanoscale materials like nanofibers, nanowires, nanorods and nanotubes have attracted superior concentration among researchers because of their potential scientific and technological applications owing to their large surface area per unit mass, smaller pore size and low basis weight [11,12].

Recently, electrospun camphorsulfonic acid doped poly (o-toluidine)-polystyrene composite fibers were used effectively as chemical vapor sensors [13]. Electrical and photovoltaic properties of cobalt doped zinc oxide nanofibers/n-silicon diode were studied [14]. Carbon nanofiber/$LiFePO_4$ composites were effectively used as Li-ion batteries [15]. Electrospun carbon/CdS coaxial nanofibers were found to exhibit photoluminescence and conductive properties [16]. Due to the electrochemical characteristics of activated carbon nanofibers, they are used as electrodes for super capacitors [17]. Nanocomposite materials are desirable due to their compliant nature in the design of prolific electronic devices [18,19].

Several novel nanofibers such as ZnO/SnO_2, nickel/carbon, TiO_2, copper oxide and ZnO/ZnS have been successfully synthesized by the twinning of sol–gel and electrospinning processes [20–24]. In our earlier work, we have reported the synthesis of ZnO nanofibers by using the same method [25]. In the present work, we have synthesized ZnO/CuO nanofibers and characterized them by X-ray diffraction (XRD), SEM, Fourier transform infrared spectroscopy (FTIR), energy dispersive X-ray analysis (EDX), UV and studied their dielectric and non-linear optical properties.

2. Experimental

2.1. Materials

Poly(vinyl alcohol) (PVA) (MW = 125,000), zinc acetate dihydrate extra pure and copper acetate purchased from Merck were used without further purification. Deionised water was used as solvent.

2.2. Methods

2.2.1. Preparation of PVA/copper acetate/zinc acetate composite sol

1.2 g of copper acetate was dissolved in 10 mL of deionised water and added to 30 g aqueous PVA solution (about 10 wt%) with constant stirring at 60 °C for 1 h. 10 mL of deionised water was added to 1.2 g of zinc acetate and then slowly added into the already prepared copper acetate/PVA solution. To this solution 6 mL of ethanol and 0.5 mL acetic acid were added while stirring. Acetic acid prevents precipitation and acts as hydrolysis/condensation catalyst. The above prepared solution was stirred for 6 h keeping in a water bath maintained at 50 °C. A viscous,

* Corresponding author. Tel.: +91 44 26811499; fax: +91 44 26811009.
E-mail address: suresrath@yahoo.com (P. Sureshkumar).

0925-8388/$ – see front matter © 2010 Elsevier B.V. All rights reserved.
doi:10.1016/j.jallcom.2010.07.161

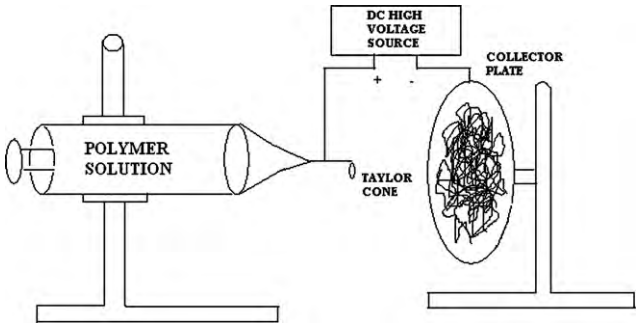

Fig. 1. Electrospinning apparatus.

clear sol solution of PVA/zinc acetate/copper acetate was obtained and used in the electrospinning process.

2.2.2. Preparation of nanofibers

The electrospinning apparatus consists of a hypodermic needle filled with 2 mL of precursor PVA/zinc acetate/copper acetate composite viscous sol gel solution. The metallic tip of hypodermic syringe needle is connected to the positive terminal of the high voltage DC generator (10–40 kV) and the negative of the generator is connected to a grounded collector as shown in Fig. 1. The aluminium sheet which is used to collect the nanofibers is fastened to the grounded metal plate by using a double-sided tape. By applying a high potential difference between the terminals, the positively charged gel is ejected from the syringe due to the attraction from the oppositely charged target, resulting in a jet. Whenever the applied voltage overcomes the surface tension of the gel which is termed as the threshold voltage, a Taylor cone is formed and the gel elongates towards the target in a whipping motion. The threshold voltage (V_c) at which the fibers are formed is directly proportional to the distance between the terminals (H). When the distance increases, the threshold voltage required is also increased as per the relation $V_c^2 \propto H^2$ [11]. Above the threshold voltage, finer fibers are obtained by lowering the applied voltage.

The electrodes were placed at a distance of 12 cm apart and by applying a high DC voltage of 13 kV between the terminals, a fluid jet was ejected from the syringe needle. Whenever the positively charged jet was accelerated towards the cathode, the solvent evaporated and a charged fiber was deposited on the aluminium foil fixed on the cathode. The formed fibers were dried for 10 h at 75 °C under vacuum and then calcined for 6 h at a temperature of 600 °C. The apparatus was kept in an isolated place which is electrically insulated and free of air current.

3. Characterization

To observe the surface topography and cross-section of the nanofibers, scanning electron microscopy images were captured using a JEOL GSM-5900 scanning electron microscope. The phase composition of the prepared samples were studied from the powder XRD patterns of the samples observed by a Rigaku D/max-A diffractometer fitted with CuKα radiation (λ = 1.5406 Å) at a scan speed of 0.01°/s at room temperature. The intensity data was recorded by continuous scan in $2\theta/\theta$ mode from 10° to 70°. Fourier Transform Infrared spectra were obtained on PerkinElmer Spectrum One, Fourier transform infrared spectrometer using KBr pellet technique. To determine the elemental composition, energy dispersive X-ray analysis was performed by using EDX, Inca, Oxford. UV spectra were obtained by using VARIAN CARY 5E spectrophotometer. Pellets of ZnO/CuO composite powders of thickness 0.79 and 12.5 mm diameter were made by applying a pressure of 4 ton in a hand operated hydraulic press. HIOKI 3532-50 LCR HITESTER meter was used to take the dielectric measurements with respect to frequency at different temperatures. The laser second harmonic generation of the sample was tested by Kurtz–Perry powder technique. The sample was illuminated by an Nd:YAG laser with modulated radiation of wavelength 1064 nm with pulse energy of 4.9 mJ/pulse, pulse width of 8 ns and repetition rate of 10 Hz. Same input was given to the potassium dihydrogen orthophosphate (KDP) reference sample.

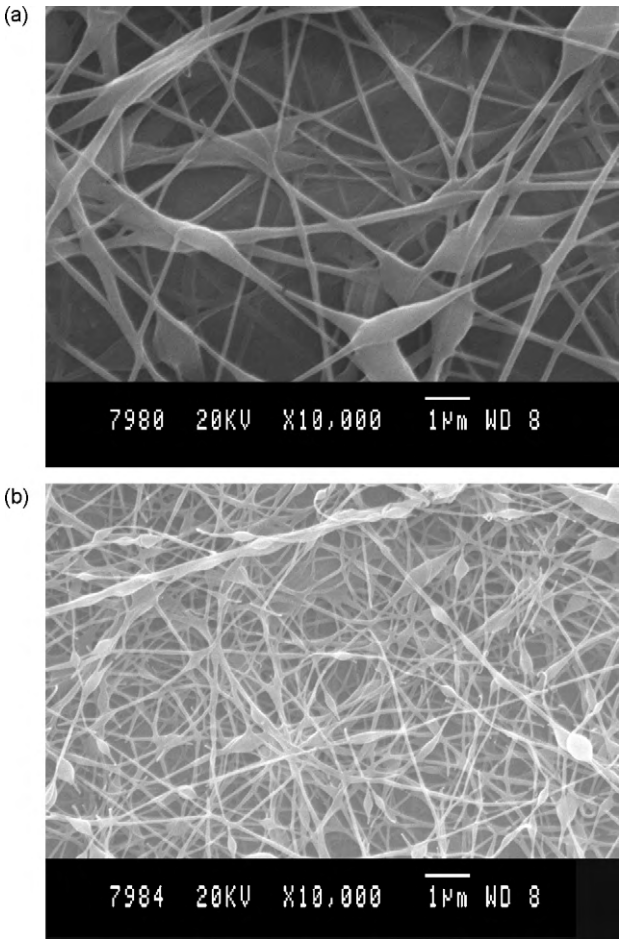

Fig. 2. (a) SEM image of synthesized nanofibers. (b) SEM image of nanofibers calcined at 600 °C.

4. Results and discussion

4.1. Scanning electron microscopy (SEM)

The SEM image of PVA/zinc acetate/copper acetate composite fibers before calcination is shown in Fig. 2(a). This micrograph shows the general topography of the synthesized fibers. The average diameter of these fibers is found to be 200 nm. The long electrospun nanofibers exhibited a cylindrical morphology with uniform thickness and were distributed in a fibrous mat. The PVA/zinc acetate/copper acetate composite fibers were calcined at 600 °C in air. After calcining, CuO is the secondary phase because it occupies the interstitial spaces in the primary phase of ZnO. Due to the removal of the organic species, the diameters of the fibers were reduced. The SEM image of the calcined fibers is shown in Fig. 2(b). The diameters of the fibers were found to vary between 50 and 100 nm. The reduction in fiber diameter is attributed mainly due to the removal of PVA and the CH_3COO^- groups of zinc acetate and copper acetate at elevated temperatures.

4.2. Powder X-ray diffraction analysis (XRD)

Fig. 3(a) shows the powder XRD pattern of the prepared fiber sample. Fig. 3(b) shows the powder XRD pattern of the fibers calcined at 600 °C. From this figure, it is clearly seen that the semi-crystalline peak of PVA found around 20° as seen in Fig. 3(a) corresponding to (1 0 1) plane [26] disappeared. XRD spectra of the fibers after calcining at 600 °C showed peaks

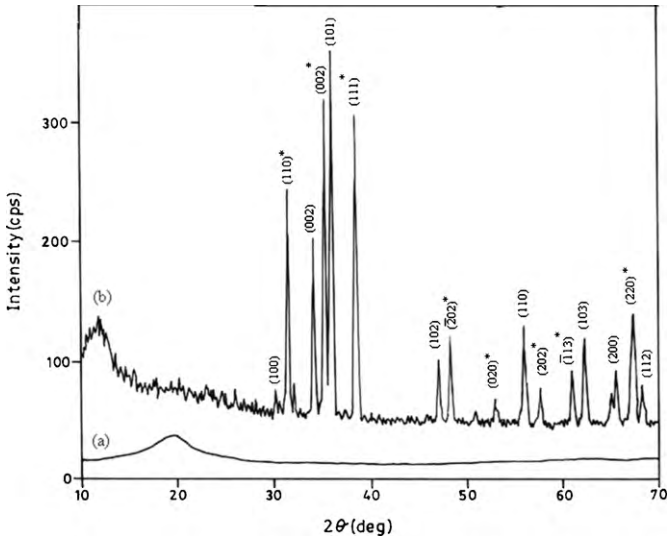

Fig. 3. (a) FTIR spectrum of the PVA/zinc acetate/copper acetate. (b) FTIR spectrum of fibers calcined at 600 °C.

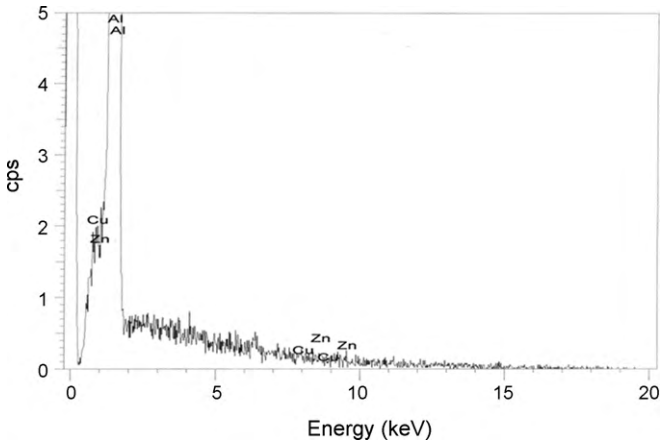

Fig. 5. EDX spectra of the calcined nanofibers.

at 31.6°(100), 34.3°(002), 36.1°(101), 47.2°(102), 56.2°(110), 62.4°(103), 65.8°(200) and 68.5°(112) corresponding to ZnO and 32.3°(110), 35.4°(002), 38.5°(111), 48.5°($\bar{2}$02), 53.1°(020), 57.9°(202), 61.1°($\bar{1}$13) and 67.5°(220) corresponding to CuO agreed very well with the literature [24,23]. The asterisk (*) marked in Fig. 3(b) denotes the CuO phases. The peaks in Fig. 3(b) could be indexed to the hexagonal wurtzite zinc oxide and monoclinic copper oxide phases separately which are in very good agreement with reported values in the literature [24,23].

4.3. FTIR analysis

Fig. 4(a) shows the FTIR spectrum of the PVA/zinc acetate/copper acetate composite fibers. Observations from Fig. 4(a) show a peak at 3401 cm^{-1} corresponding to the alcoholic stretching vibrations of –OH. The bands at 1648 and 1284 cm^{-1} should attribute to the C=O and C–O stretching vibrations of the carboxyl groups respectively. The band at 1416 cm^{-1} is attributed to the C–H alkane scissoring and bending vibrations. The band at 1100 cm^{-1} corresponds to the C–O bending. A band at 2139 cm^{-1} is attributed to C=C stretching and another band at 743 cm^{-1} corresponds to –CH out of plane bending. No band is found between 1500 and 1600 cm^{-1} corresponding to the typical bending frequencies of –OH. This could be interpreted that the as-synthesized fibers were dry. After calcining, a new overlapped peak around 531 cm^{-1} is observed in the FTIR spectrum and is assigned to ν_{Cu-O}[23] and ν_{Zn-O} [27] and all the other peaks disappeared as shown in Fig. 4(b). These results confirm the complete removal of organic molecules from PVA/zinc acetate/copper acetate composite fibers after calcining at 600 °C, and the fibers obtained after calcinations at this temperature are pure ZnO/CuO inorganic species.

4.4. Energy dispersive X-ray (EDX) analysis

EDX spectrum of the calcined ZnO/CuO nanofibers is shown in Fig. 5 confirms the presence of the compounds CuO and ZnO in the ratio of 41.9% and 58.1%, respectively. The EDX spectrum shows a greater peak for the Al_2O_3 sheet which was used to collect the nanofibers.

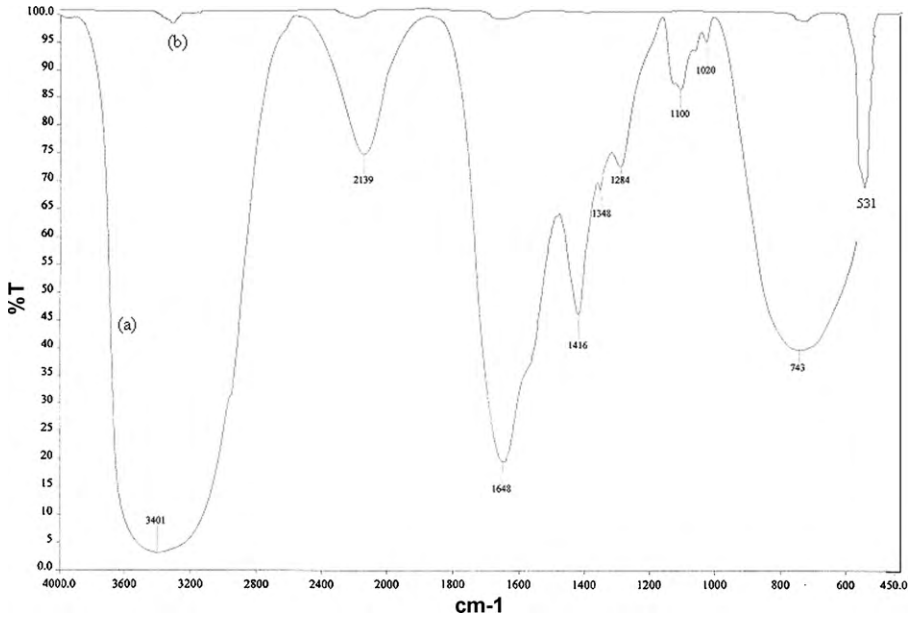

Fig. 4. (a) XRD pattern of the synthesized fibers. (b) XRD pattern of nanofibers calcined at 600 °C.

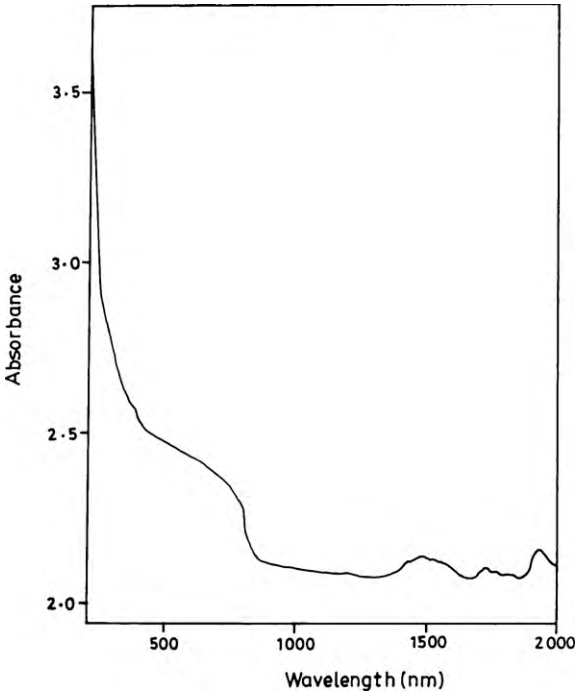

Fig. 6. UV spectra of the ZnO/CuO nanocomposite.

4.5. Optical absorption studies

The optical absorption spectrum of ZnO/CuO nanocomposite was recorded in the wavelength region of 200–2000 nm and is shown in Fig. 6. The very low absorption property of the synthesized fiber in the entire visible region suggests its suitability for second harmonic generation [28,29]. The UV absorption edge of the ZnO/CuO nanocomposite is observed to be around 240 nm. The dependence of optical absorption coefficient with the photon energy helps to study the band structure and the type of transition of electrons.

As a direct band gap material, the nanocomposite under study has an absorption coefficient (α) obeying the following relation for high photon energies ($h\nu$):

$$\alpha = \frac{A(h\nu - E_g)^{1/2}}{h\nu}$$

where E_g is optical band gap of the nanocomposite and A is a constant. From the plot of $(\alpha h\nu)^2$ vs $h\nu$ shown in Fig. 7, band gap energy E_g is evaluated by the extrapolation of the linear part [30]. The band gap is found to be 3.1 eV and the comparison of band gap energy of ZnO/CuO nanocomposite material with similar type of materials is given in Table 1.

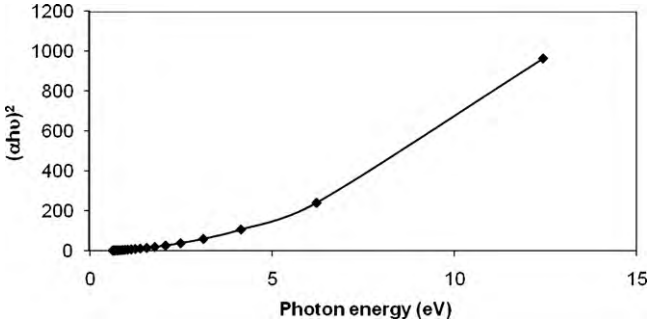

Fig. 7. Plot of variation of $(\alpha h\nu)^2$ vs $h\nu$.

Table 1
Comparison of Band gap energy.

Name of the material	Bandgap energy (eV)
ZnO/CuO nanocomposite	3.1
ZnO	3.3
CuO	2.78

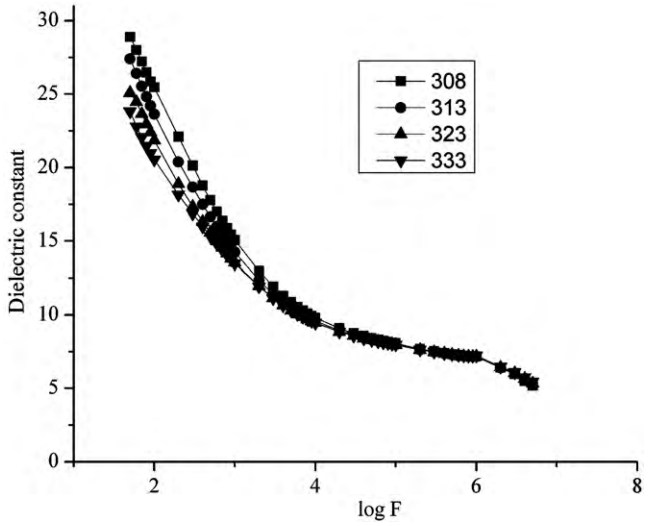

Fig. 8. log F vs dielectric constant.

4.6. Dielectric studies

The dielectric constant (ε') of the nanocomposite sample was determined by using the relation

$$\varepsilon' = \frac{Cd}{\varepsilon_0 A}$$

where C is the capacitance, d is the thickness, ε_0 is the permitivity of the free space (8.854×10^{-12} F/m) and A is the surface area of the sample.

The variation of dielectric constant (ε') was studied as a function of frequency for the nanocomposite materials at various temperatures viz., 308, 313, 323 and 333 K and is shown in Fig. 8. The dielectric constant has high values in the low frequency regions for

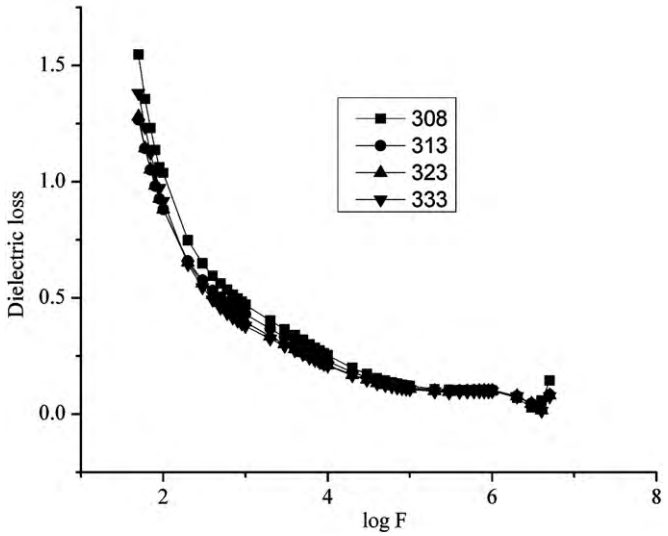

Fig. 9. log F vs dielectric Loss.

Table 2
Comparison of SHG efficiency of ZnO/CuO with other materials.

Compound name	SHG efficiency compared with KDP	Reference
ZnO/CuO nanocomposite	11 times	Present work
Urea	7.5 times	Present work
ZnO nanorod arrays	11.3 times	[34]

the nanomaterials than for the conventional materials. The very high values of dielectric constant at low frequencies may be due to the presence of different types of polarization mechanisms [31]. Because of the presence of interfaces in the nanomaterials, the application of an electric field creates dipole moments and rotates them along the applied field direction which is called as rotation direction polarization. Space charge polarization and rotation direction polarization are responsible for the high value of dielectric constant for nanomaterials at low frequencies [32].

The variation of dielectric loss was also studied as a function of frequency for calcined materials at various temperatures viz. 308, 313, 323 and 333 K and is shown in Fig. 9. It is evident that for all temperatures the dielectric loss decreases with increase in the frequency. This suggests that the dielectric loss is strongly dependent on the frequency of the applied field. Low dielectric loss indicates the very high purity of the synthesized materials, having lesser defects with enhanced optical quality [33]. Decrease in the dielectric constant and dielectric loss of the nanocomposite with respect to increase in the frequency suggests that this material can be employed in the fabrication of devices used at high frequencies.

4.7. Non-linear optical studies

The second harmonic generation efficiency measurement was carried out on the ZnO/CuO nanocomposite with reference to KDP and urea by using the Kurtz–Perry powder technique. The laser power was kept constant throughout the experiment. The doubling of the input frequency was confirmed by illuminating the sample by using an Nd:YAG laser of wavelength 1064 nm producing an output of green wavelength of 532 nm. The output power is found to be 11.1 times that of KDP and 1.5 times that of urea. The comparison of the SHG efficiency of the ZnO/CuO composite with similar materials is given in Table 2. ZnO/CuO is a potential nanocomposite material for the light conversion and for the development of non-linear optical devices using nanocomposites.

5. Conclusions

ZnO/CuO composite nanofibers were synthesized by electrospinning of the PVA/zinc acetate/copper acetate precursor and by subsequent calcination. The fibers were characterized by SEM, XRD, FTIR, EDX and UV, respectively. The fiber diameters were found to vary between 50 and 100 nm. Dielectric constant and dielectric loss of the sample decreases with increase in frequency. The second harmonic efficiency is found to be 11.1 times that of KDP and 1.5 times that of urea. Electrospinning would be a promising approach for the large scale synthesis of one dimensional ZnO/CuO nanocomposites for prolific practical applications.

Acknowledgements

The authors wish to express their thanks to the Department of Nuclear Physics, Madras University for X-ray studies, Dr. P.K. Das, Indian Institute of Science for the NLO studies and SAIF, IIT, Madras for the experimental facilities. The stimulating discussion with Dr. S. Krishnan and Mr. D. Nedumaran of R.M.K. Engineering College is gratefully acknowledged.

References

[1] A.A. Farghali, M. Moussa, M.H. Khedr, J. Alloys Compd. 499 (2010) 98–103.
[2] N.M. Deraz, J. Alloys Compd. 501 (2010) 317–325.
[3] Li-Dong Zhao, Bo-Ping Zhang, Jing-Feng Li, Min Zhou, Wei-Shu Liu, Jing Liu, J. Alloys Compd. 455 (2008) 259–264.
[4] P.G. Li, M. Lei, W.H. Tang, X. Guo, X. Wang, J. Alloys Compd. 477 (2009) 515–518.
[5] Xiaorui Hou, Shengming Zhou, Yukun Li, Wenjie Li, J. Alloys Compd. 494 (2010) 382–385.
[6] S. Capula Colindres, J.R. Vargas García, J.A. Toledo Antonio, C. Angeles Chavez, J. Alloys Compd. 483 (2009) 406–409.
[7] A. Azizi, S.K. Sadrnezhaad, J. Alloys Compd. 485 (2009) 484–487.
[8] Deyi Wang, Jian Zhou, Guizhen Liu, J. Alloys Compd. 487 (2009) 545–549.
[9] C.-H. Lu, B. Bhattacharjee, S.-Y. Chen, J. Alloys Compd. 475 (2009) 116–121.
[10] M. Escobar, L. Giuliani, R.J. Candal, D.G. Lamas, A. Caso, G. Rubiolo, D. Grondona, S. Goyanes, A. Márquez, J. Alloys Compd. 495 (2010) 446–449.
[11] Zheng-Ming Huang, Y.-Z. Zhang, M. Kotaki, S. Ramakrishna, Compos. Sci. Technol. 63 (2003) 2223–2253.
[12] Ioannis S. Chronakis, J. Mater. Process. Technol. 167 (2005) 283–293.
[13] D. Aussawasathien, S. Sahasithiwat, L. Menbangpung, Synth. Met. 158 (2008) 259–263.
[14] Fahrettin Yakuphanoglu, J. Alloys Compd. 494 (2010) 451–455.
[15] M.S. Bhuvaneswari, N.N. Bramnik, D. Ensling, H. Ehrenberg, W. Jaegermann, J. Power Sources 180 (2008) 553–560.
[16] Y. Yang, H. Wang, X. Lu, Y. Zhao, X. Li, C. Wang, Mater. Sci. Eng. B 140 (2007) 48–52.
[17] M.-K. Seo, S.-J. Park, Mater. Sci. Eng. B 164 (2009) 106–111.
[18] S.-D. Kim, H. Moon, S.-H. Hyun, J. Moon, J. Kim, H.-W. Lee, J. Power Sources 163 (2006) 392–397.
[19] W. Mekprasart, W. Jarernboon, W. Pecharapa, Mater. Sci. Eng. B 172 (2010) 231–236.
[20] R. Liu, Y. Huang, A. Xiao, H. Liu, J. Alloys Compd. 503 (2010) 103–110.
[21] Jian Li, En-hui Liu, Wen Li, Xiang-yun Meng, Song-ting Tan, J. Alloys Compd. 478 (2009) 371–374.
[22] Jianguo Zhao, Changwen Jia, Huigao Duan, Hui Li, Erqing Xie, J. Alloys Compd. 461 (2008) 447–450.
[23] Hongyu Guan, Changlu Shao, Bin Chen, Jian Gong, Xinghua Yang, Inorg. Chem. Commun. 6 (2003) 1409–1411.
[24] Yong Liu, Yufeng Song, Dairong Chen, Xiuling Jiao, Wenxing Zhang, J. Dispers. Sci. Technol. 27 (2006) 1191–1195.
[25] R. Siddheswaran, R. Sankar, M. Ramesh Babu, M. Rathnakumari, R. Jayavel, P. Murugakoothan, P. Sureshkumar, Cryst. Res. Technol. 41 (2006) 446–449.
[26] Y. Nishio, R.S.J. Manley, Macromolecules 21 (1988) 1270–1277.
[27] Y.J. Kwon, K.H. Kim, C.S. Lim, K.B. Shim, J. Ceram. Process. Res. 3 (2002) 146–149.
[28] S. Anie Roshan, Cyriac Joseph, M.A. Ittyachen, Mater. Lett. 49 (2001) 299–302.
[29] V. Venkataramanan, S. Maheswaran, J.N. Sherwood, H.L. Bhat, J. Cryst. Growth 179 (1997) 605–610.
[30] A.K. Chawla, D. Kaur, R. Chandra, Opt. Mater. 29 (2007) 995–998.
[31] C.-M. Mo, L. Zhang, G. Wang, Nanostruct. Mater. 6 (1995) 823–826.
[32] N.J. Tharayil, R. Raveendran, A. Varghese Vaidyan, P.G. Chithra, Indian J. Eng. Mater. Sci. 15 (2008) 489–496.
[33] C. Balarew, R. Duhlev, J. Solid State Chem. 55 (1984) 1–6.
[34] Z. Gui, X. Wang, J. Liu, S. Yan, Y. Ding, Z. Wang, Y. Hu, J. Solid State Chem. 179 (2006) 1984–1989.